Recent Advances in Measurement and Modeling of Electron Cloud Buildup at CESR and Predictions for CHESS-U

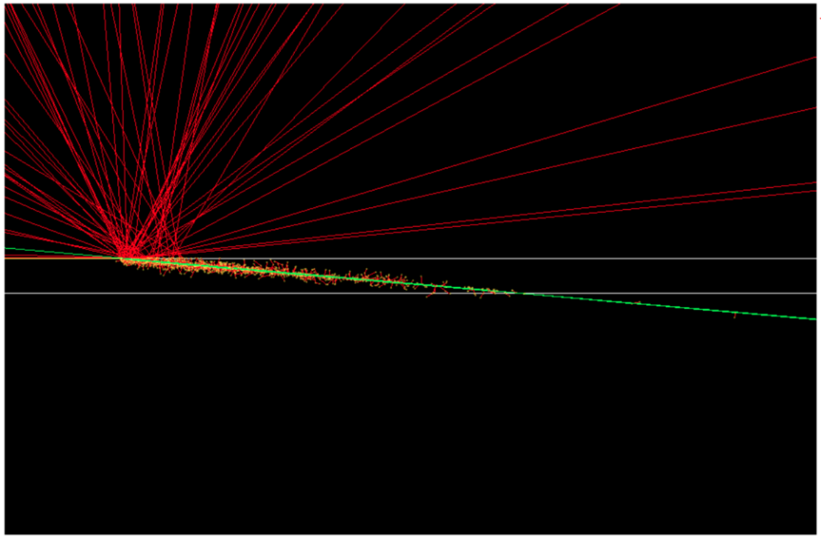

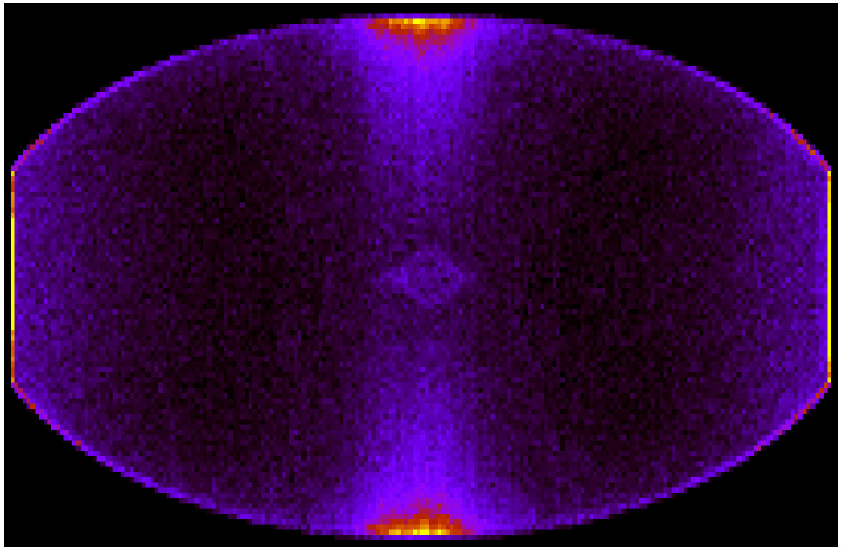

Jim Crittenden and Stephen Poprocki

CLASSE Seminar

Wilson Synchrotron Laboratory

2 August 2018

Part 1 (JAC)

Simulations of synchrotron-radiation-induced electron production in the CESR vacuum chamber wall

Part 2 (STP)

Measurements and model validation of electron-cloud-induced betatron tune shifts in the CESRTA, CHESS and CHESS-U transition lattices and predictions for CHESS-U operation

Electron cloud since the 1960's

F. Zimmerman overview talk at ECLOUD12

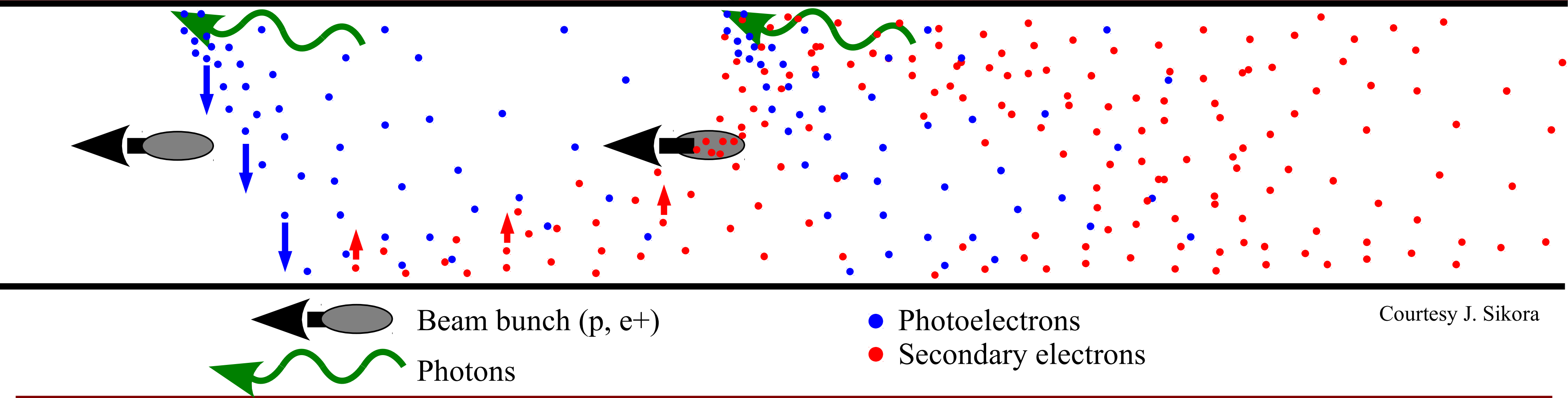

Topical worldwide since the mid-1990s

1) Identified as the source of instabilities in the positron rings of the B-factories PEP-II and KEKB, leading to extensive post-design mitigation strategies

2) Recognition that synchrotron radiation rates at the LHC are comparable to those in positron rings because of the high proton energy (7 TeV). Cryo load now at capacity.

(Retroactively recognized as the likely source of hitherto mysterious instabilities observed in storage rings since the 1960s)

Topical at CESR since 2007

1) The CESRTA project tasked with developing mitigation strategies for the positron damping ring of the International Linear Collider (JAC et al, Phys. Rev. ST Accel. Beams 17, 031002 (2014))

2) The CHESS-U project designed to begin operation with a single positron beam

Cloud-induced distortions of the beam optics

- **The space-charge electric field of the cloud acts like an electrostatic lens. A positively charged beam attracts cloud into the beam bunches, resulting in a focusing effect in both horizontal and vertical planes, increasing the betatron tunes above those defined by the design optics, i.e. by the quadrupole magnet settings.**
- **Precise measurements of the change in tune provide information on the density profile of the cloud integrated over the orbit around the ring.**
- **This density profile evolves in a complicated way along the length of a train of beam bunches, requiring sophisticated numerical modeling. The comparison of modeled and measured tunes for each bunch provides a way to assess the accuracy of our model.**

Example

Effect of the chosen electron production model on the simulation calculation of the tune shifts

Left: Full electron production model described below here in Part 1

Right: Original ad hoc model in CERN simulation code(2008)

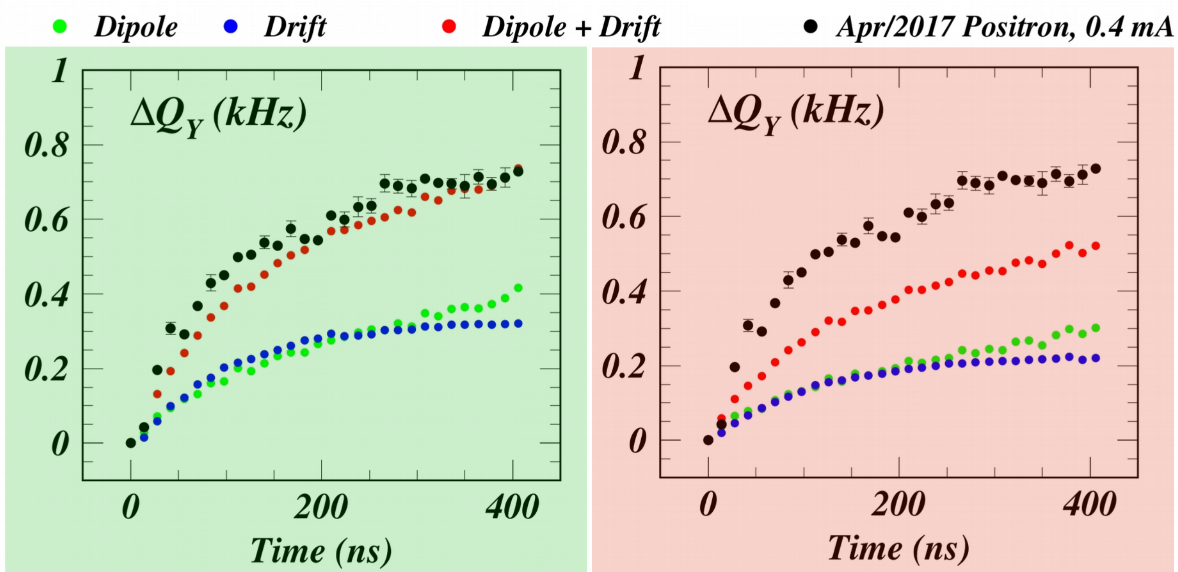

Motivation for a physical (defensible) model for electron production

- Observations and Predictions at CESRTA and Outlook for ILC, G.Dugan et al, ECLOUD12
- The CESR Test Accelerator Electron Cloud Research Program: Phase I Report, M.A.Palmer et al, CLNS-12-2084 (2013)
- Investigation into Electron Cloud Effects in the International Linear Collider Positron Damping Ring, J.A.Crittenden et al, Phys. Rev. ST Accel. Beams, Vol 17, 031002 (2014)
- J.A.Crittenden, THPAF26, IPAC18
- S.Poprocki, THPAF25, IPAC18
- Stephen Poprocki, ECLOUD18

I. Extensive CESRTA measurements of tune shifts and beam sizes in 2016 and 2017 at 2.1 and 5.3 GeV with varying bunch populations, together with improved data-taking methods and analysis techniques pointed to the need for more sophisticated modeling (see Part 2).

II. While the necessity of a detailed model of synchrotron radiation photon scattering inside the CESR beam pipe had been recognized and addressed, new information on roughness, material and coating had not been taken into account.

III. The assumptions in the electron cloud buildup model for the dependence of quantum efficiency on azimuthal absorbed photon location remained coarse and ad hoc, as did the photoelectron production energy distributions.

IV. Over the past decade, much progress in modeling low-energy atomic processes has been implemented in the CERN-maintained Geant4 Monte Carlo simulation code, driven in part by medical physics applications.

We describe here the implementation of a Geant4 postprocessor for the Cornell Synrad3D photon tracking code.

Importance of photoelectron energies

Interplay with attractive force from beam bunches

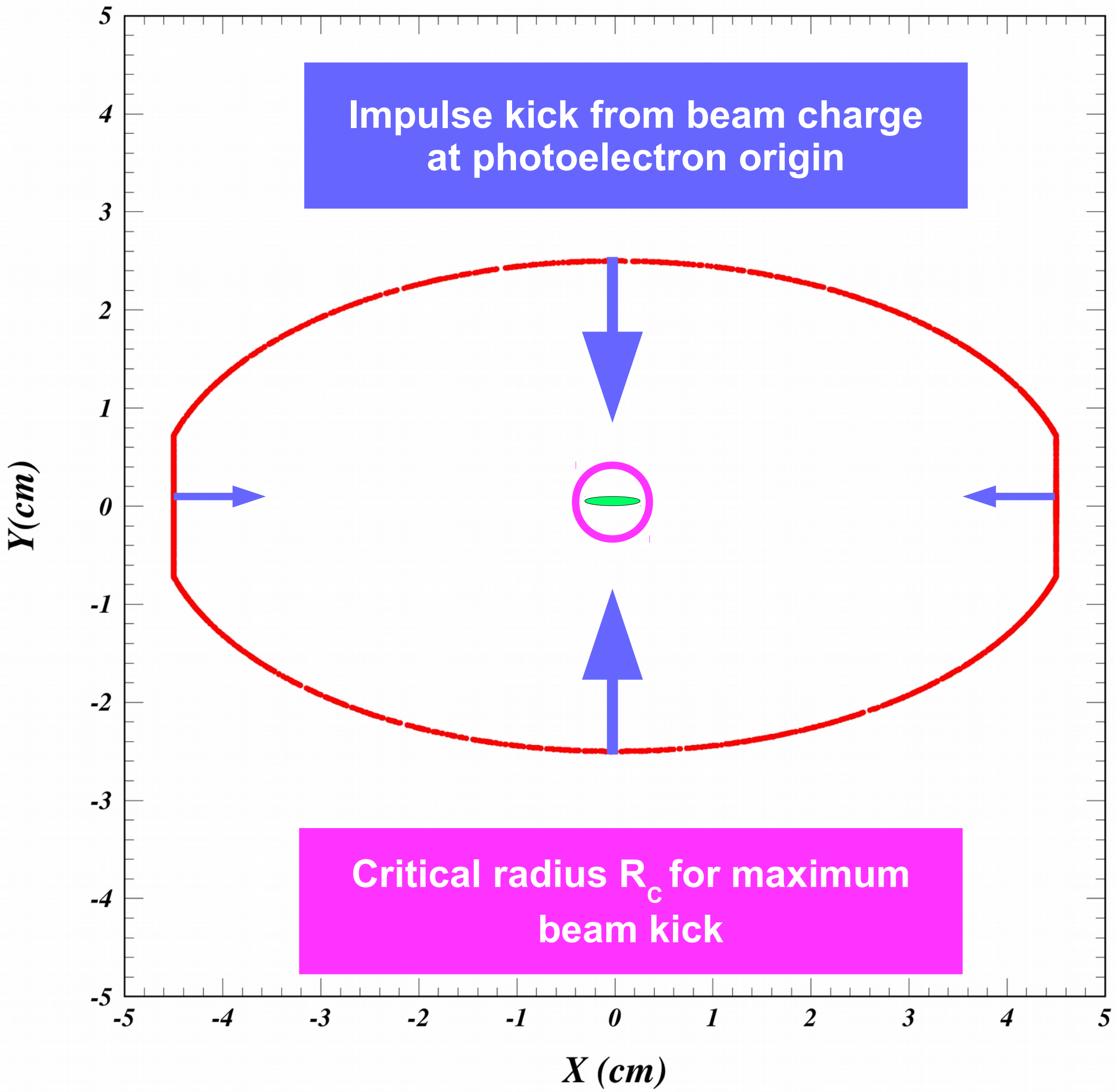

2.1 GeV

0.6e10 e+/bunch (0.4 mA)

X kick: 0.02 eV (-0.14 eV from image)

Y kick:1.10 eV (+0.50 eV from image)

R_C=9.2 mm

Max kick: 1.2 keV

5.3 GeV

9.5e10 e+/bunch (6 mA)

X kick: 4 eV (-32 eV from image)

Y kick: 235 eV (+120 eV from image)

R_C=3.7 mm

Max kick: 14 keV

9 eV: 25 mm/14 ns

36 eV: 50 mm/14 ns

Outline

I) **Photon tracking model extensions**

1) Effect of microgrooves
2) Dependence on pipe material
3) Effect of thin surface layers

II) **Modeling of electron production**

1) Photoelectric and atomic de-excitation processes
2) Dependence on beam-pipe materials

III) **Combined results input to electron cloud buildup model**

1) Electron production rate distributions
2) Electron production energy distributions

Implementation of 10-μm grooves in the CESR vacuum chamber model

Measurements of x-ray scattering from accelerator vacuum chamber surfaces, and comparison with an analytical model, G. F. Dugan, K. G. Sonnad, R. Cimino, T. Ishibashi, and F. Schäfers, Phys. Rev. ST Accel. Beams 18, 040704 (2015)

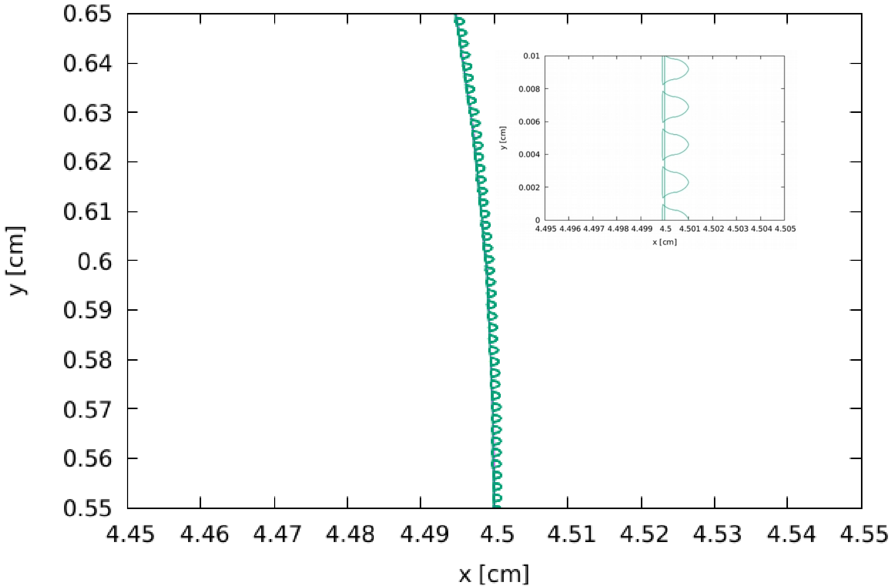

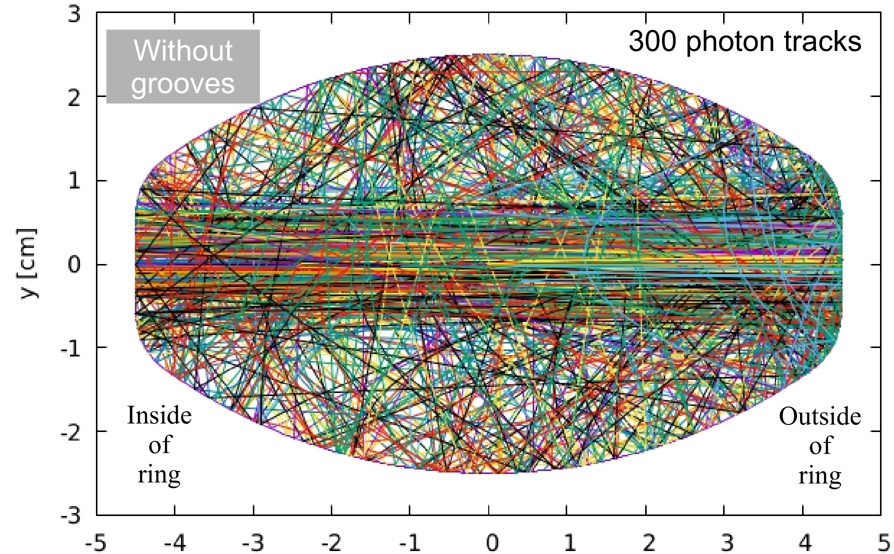

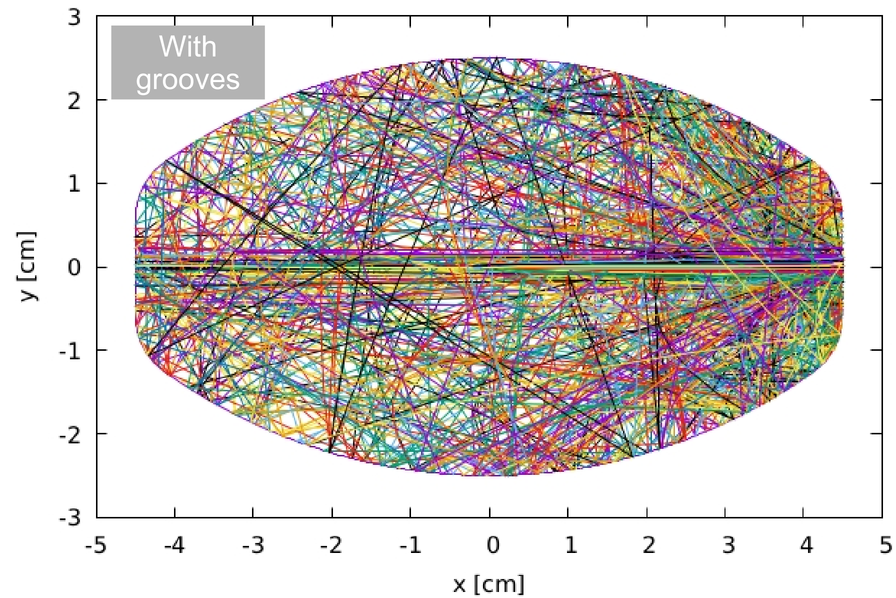

Small grooves observed in AFM measurements result in greatly enhanced out-of-plane photon scattering.

Curved trajectories in XY coordinate system result from the longitudinal pipe bend in the dipole magnet.

Azimuthal distribution of photon absorption sites on the vacuum chamber wall

Field-free regions

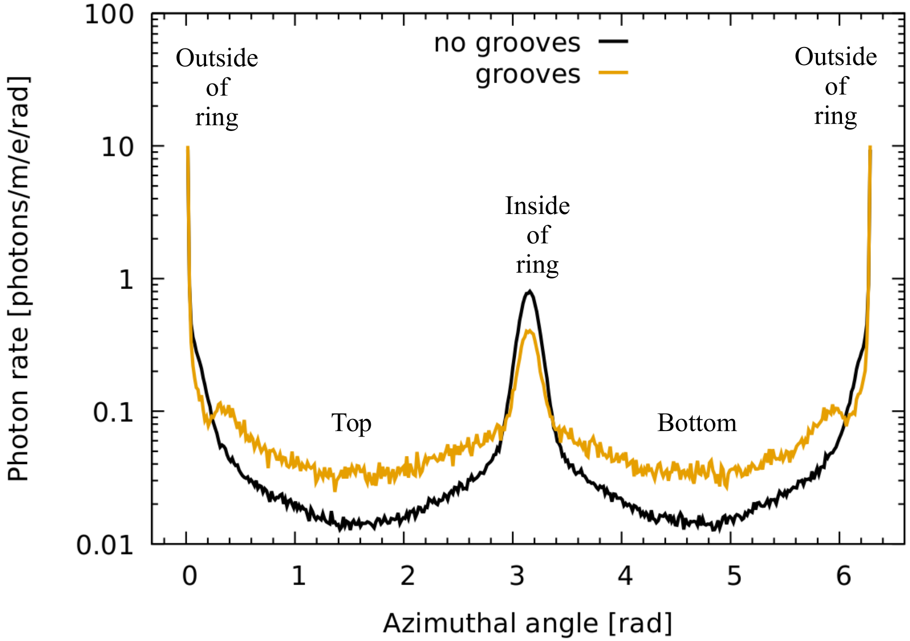

Dipole regions

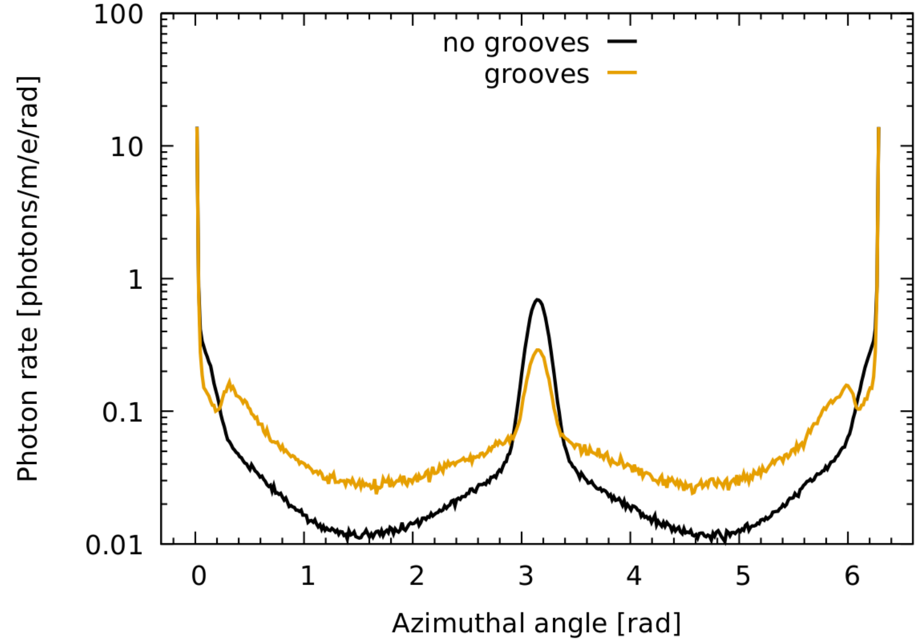

The effect of grooves is to enhance photoelectron production on the top and bottom of the beam-pipe, increasing the contribution of dipole regions to the tune shift and emittance growth calculations due to the tight spiraling of cloud electrons around the vertical magnetic field lines guiding them into the beam.

Reflectivity dependence on material

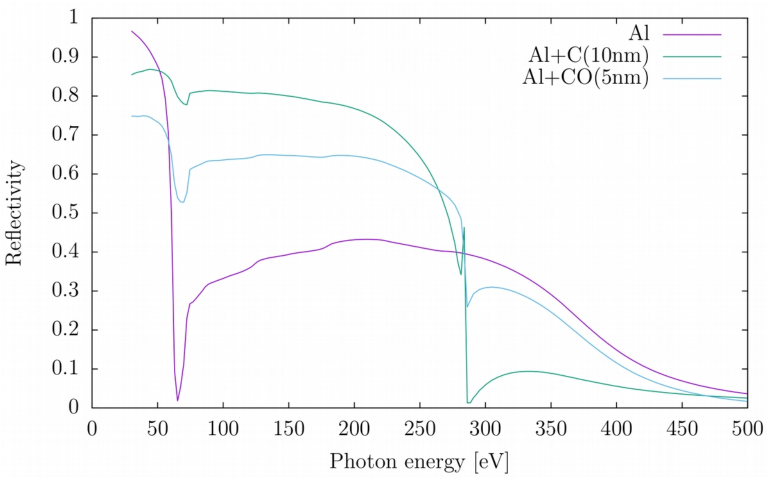

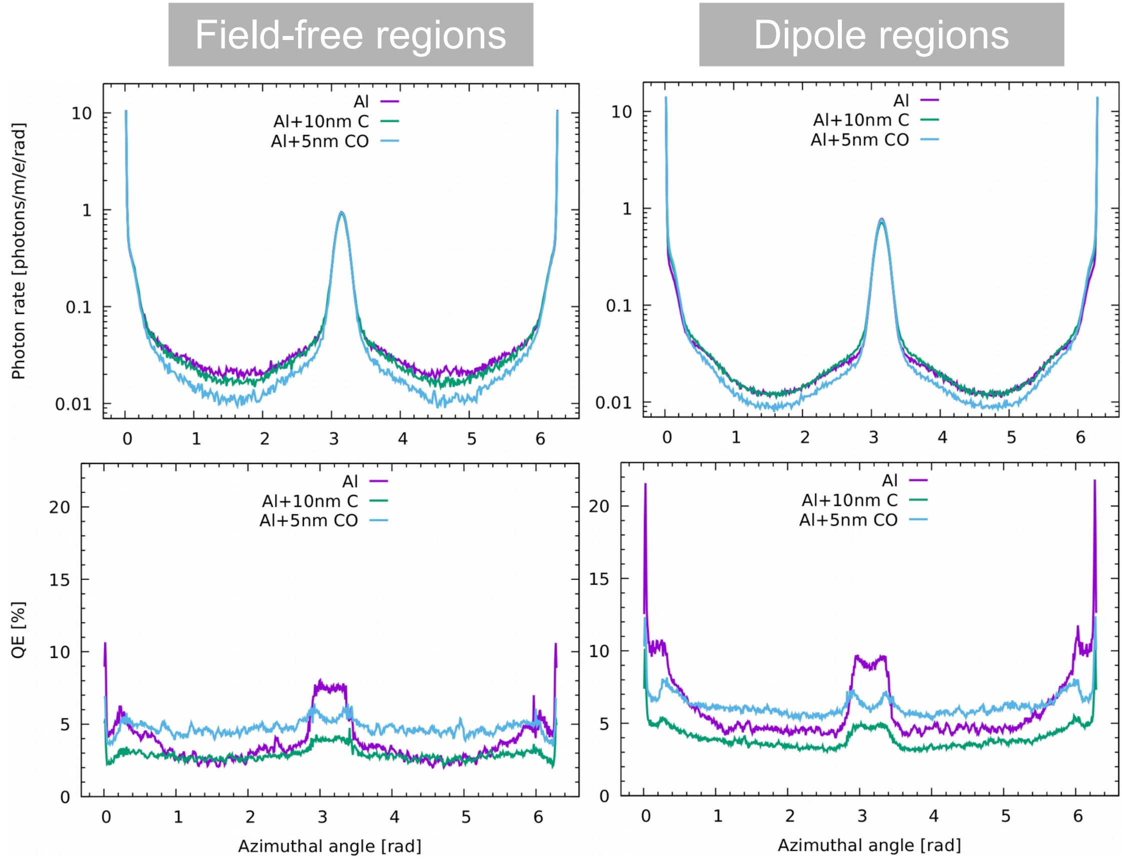

Reflectivity derived from Henke LBNL tables for various vacuum chamber surface materials

Determines photon absorption site distributions, absorbed photon energies and incident wall angles

Product of quantum efficiency and photon rate used as input to electron cloud buildup model (e-/m/e+ vs azimuthal angle)

Detailed model of CESR vacuum chamber

Cornell University
Laboratory for Elementary-Particle Physics

Simulating synchrotron radiation in accelerators including diffuse and specular reflections, G. Dugan and D. Sagan, Phys. Rev. Accel. Beams 20, 020708 (2017)

Plan view

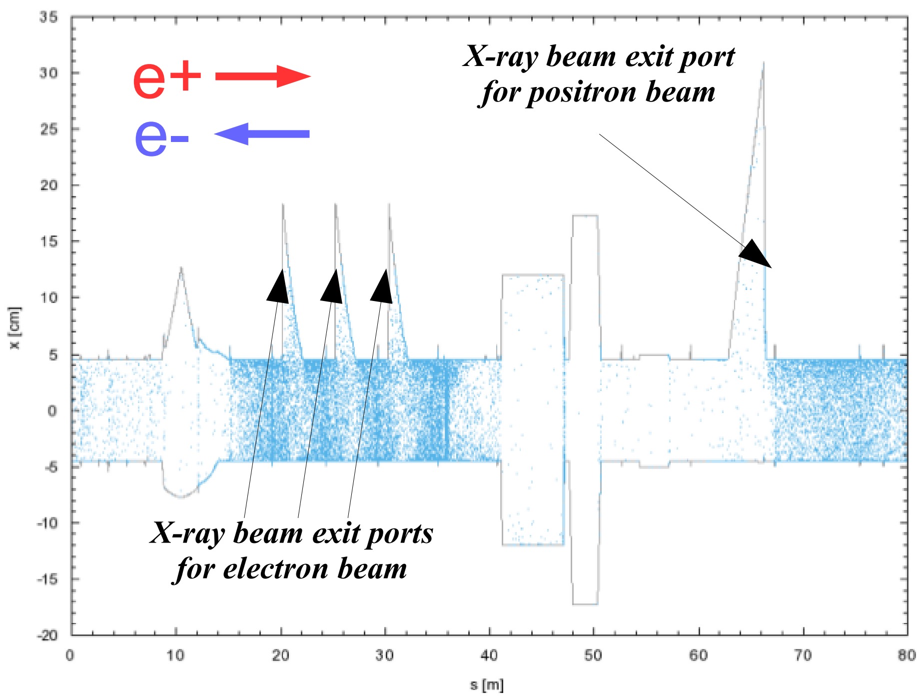

Elevation view

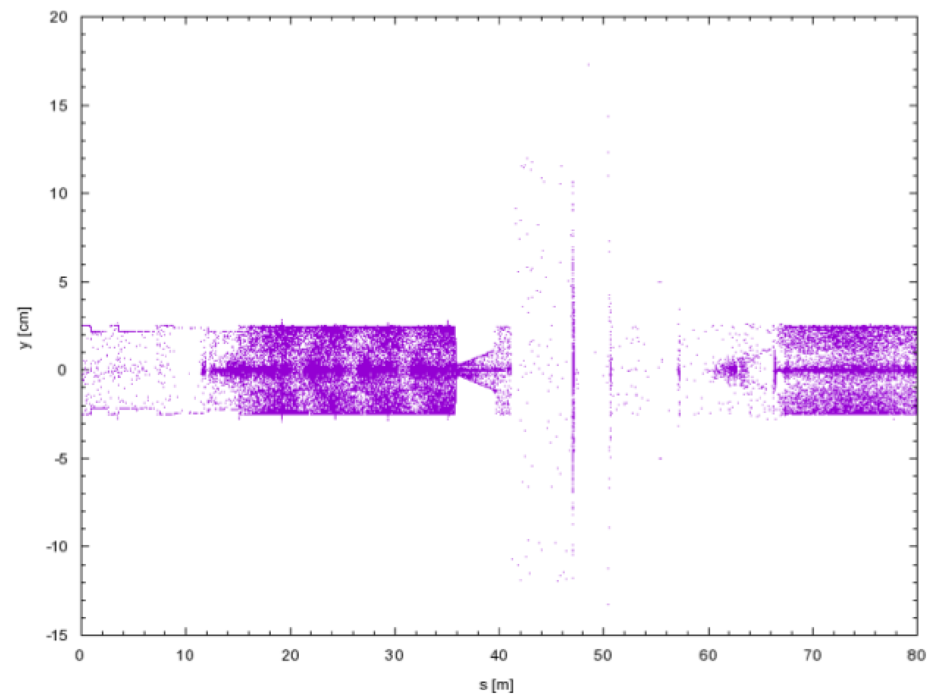

10^6 photons tracked around the 768-m CESR ring
Vacuum chamber model includes gate valves, bellows, etc

Photon tracking results
5.3 GeV e+ beam

Average absorbed photon rate: 0.78 photons/m/e

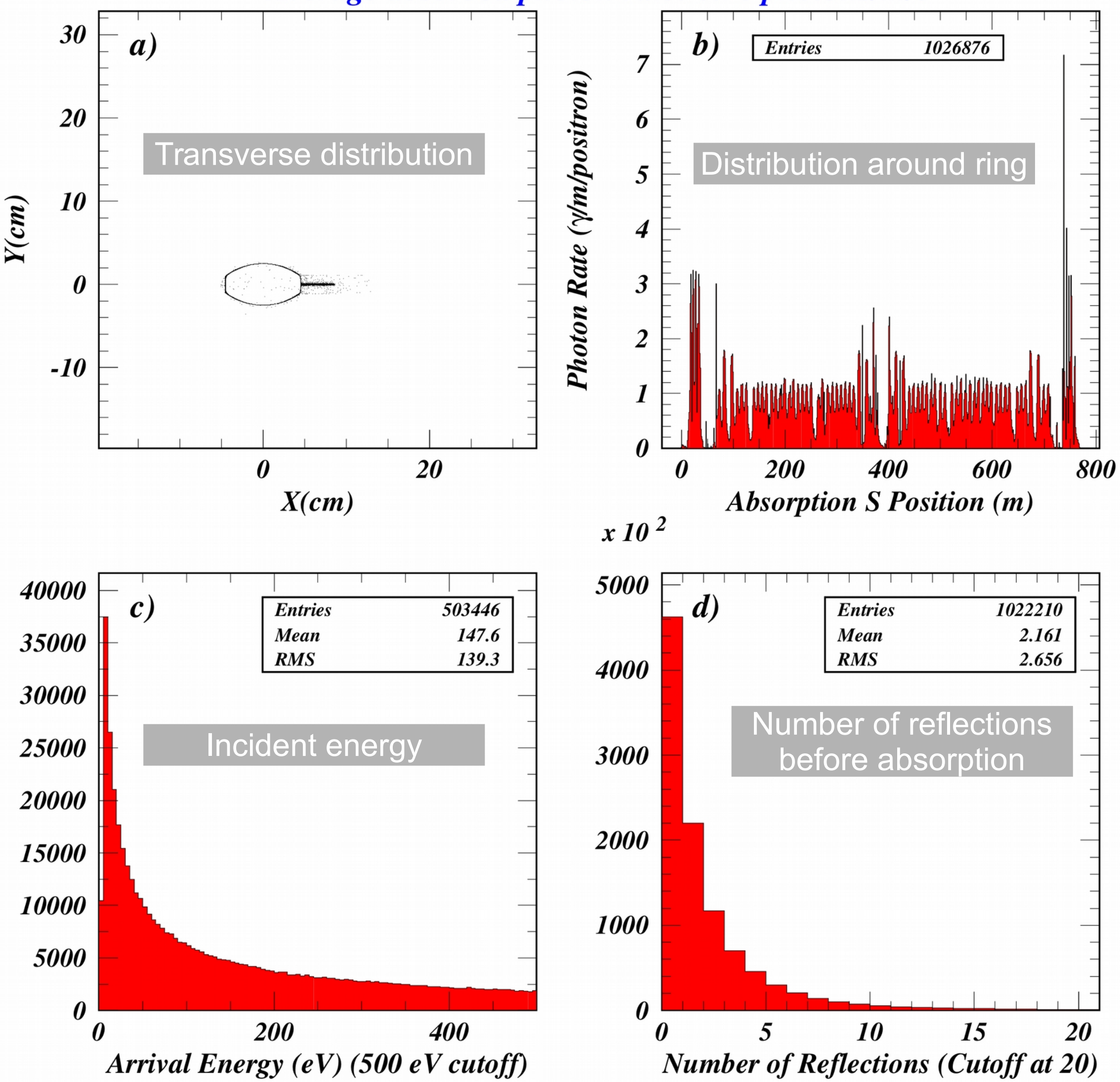

Characteristics of absorbed photons

Hot spots around ring due to vacuum chamber geometry

Diffuse scattering and many reflections result in absorption sites on top and bottom of vacuum chamber

Absorbed photon energies and grazing angles
5.3 GeV e+ beam

Photon energies

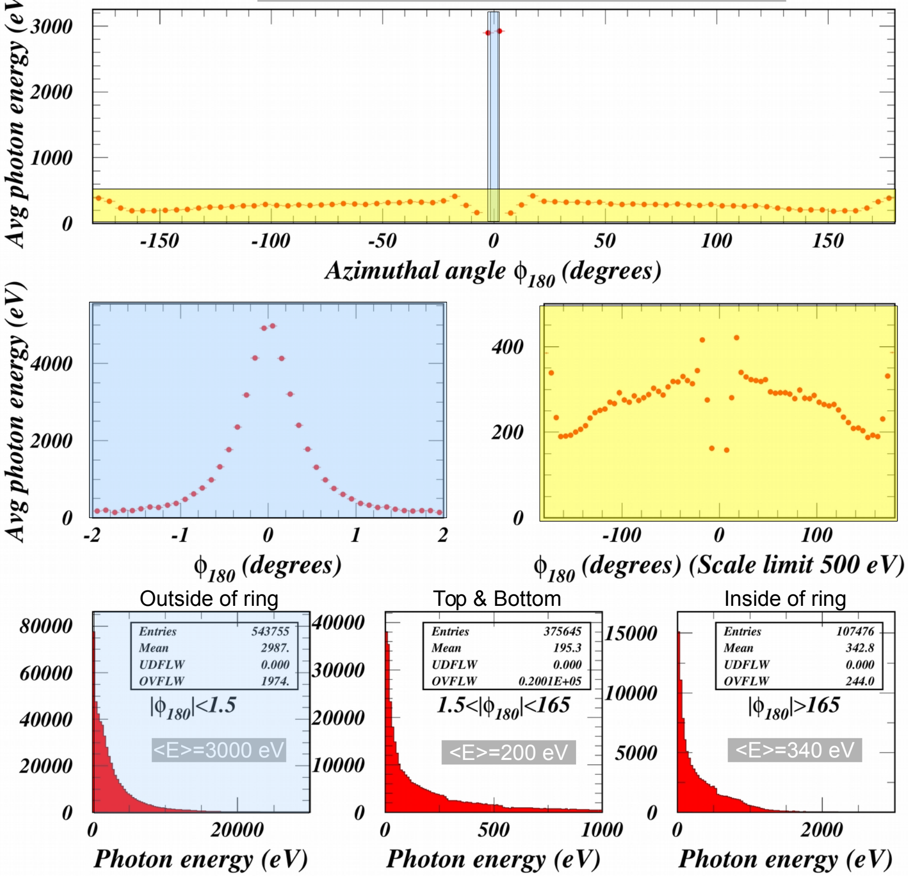

Photon incident angle

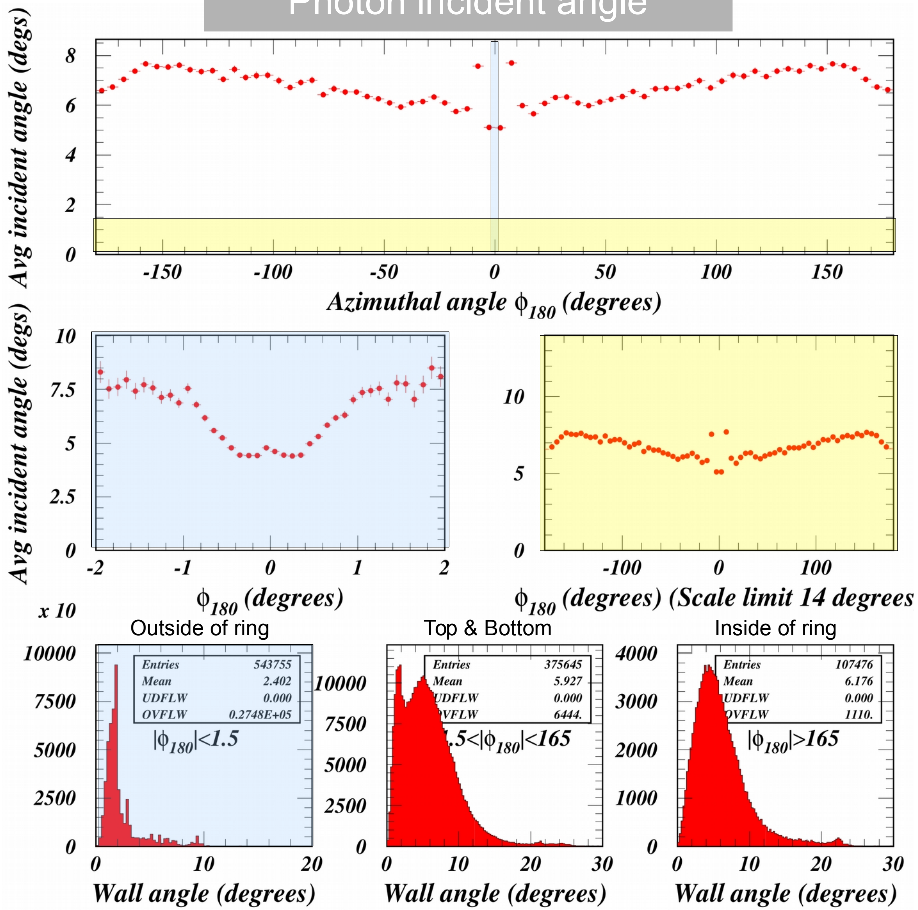

Dramatic dependence of photon energies and incident angles on azimuthal absorption location.
We distinguish three azimuthal regions for generating electron energies .
Absorption site and energy distributions are averaged over dipole and field-free regions separately for input to electron cloud buildup modeling.

QE dependence on photon energy and incident angle

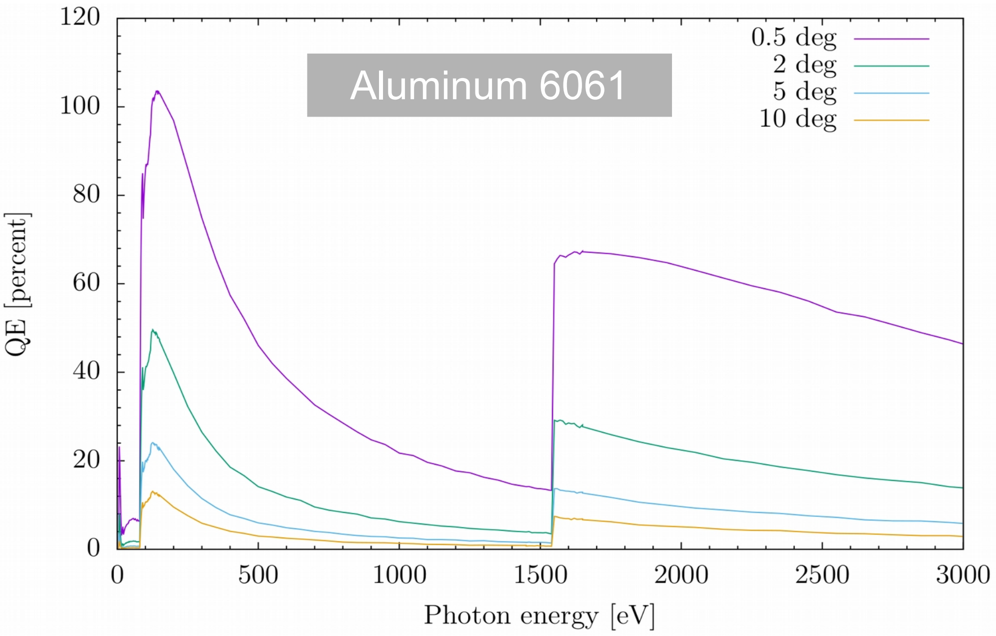

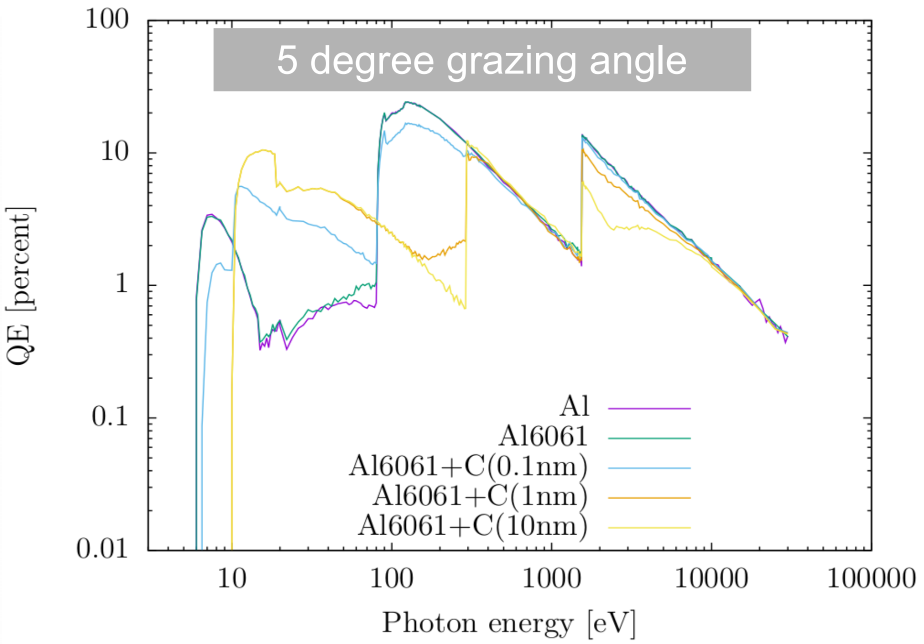

Geant4 photoabsorption cross sections show important dependence on absorbed photon energy and angle of incidence on the wall.

The photon tracking code Synrad3D provides this information on a photon-by-photon basis.

Evaluated Atomic Data Library in Geant4 -- comprehensive, detailed --

non-radiative transitions

Element	Subshells	Transition Probability	Emitted Electron (eV)
13–Al	K L1 L1	7.83944–2	1311.80
	K L1 L2	8.32180–2	1349.65
	K L1 L3	1.62725–1	1350.12
	K L1 M1	1.35884–2	1420.69
	K L1 M3	1.76485–3	1425.98
	K L2 L2	1.42920–2	1387.50
	K L2 L3	3.66942–1	1387.97
	K L2 M1	6.49294–3	1458.54
	K L2 M3	3.65883–3	1463.83
	K L3 L3	2.09226–1	1388.44
	K L3 M1	1.27063–2	1459.01
	K L3 M2	3.65189–3	1464.29
	K L3 M3	4.20421–3	1464.30
	L1 L2 M1	2.98134–1	27.6900
	L1 L2 M2	1.67498–2	32.9700
	L1 L2 M3	1.46673–2	32.9800
	L1 L3 M1	5.89896–1	28.1600
	L1 L3 M2	1.45284–2	33.4400
	L1 L3 M3	4.66786–2	33.4500
	L1 M1 M1	1.12532–2	98.7300
	L1 M1 M2	2.61944–3	104.010
	L1 M1 M3	5.21749–3	104.020
	L2 M1 M1	1.50408–1	60.8800
	L2 M1 M2	8.00076–1	66.1600
	L2 M1 M3	4.94996–2	66.1700
	L3 M1 M1	1.44757–1	60.4100
	L3 M1 M2	2.47625–2	65.6900
	L3 M1 M3	8.30465–1	65.7000

subshell parameters

Element	Subshell	Electrons per Subshell	Binding Energy (eV)	Kinetic Energy (eV)	Average Radius (milli-A)	Radiative Width (eV)	Non-Rad. Width (eV)	"Average Total Energies" Photons (eV)	Electrons (eV)	Local (eV)
13–Al	K	2.00	1549.90	2191.00	63.1760	1.38230–2	3.65180–1	54.5949	1460.64	34.6619
	L1	2.00	119.050	307.380	324.100	1.48830–5	1.38950+0	0.01128	93.7117	25.3270
	L2	2.00	81.2000	288.300	306.880	2.69150–6	5.71690–3	0.00114	65.3653	15.8336
	L3	4.00	80.7300	285.960	307.960	2.70920–6	5.71420–3	0.00105	64.9330	15.7959
	M1	2.00	10.1600	33.5300	1292.90					10.1600
	M2	0.33	4.88000	18.3800	1817.70					4.88000
	M3	0.67	4.87000	18.2400	1823.40					4.87000

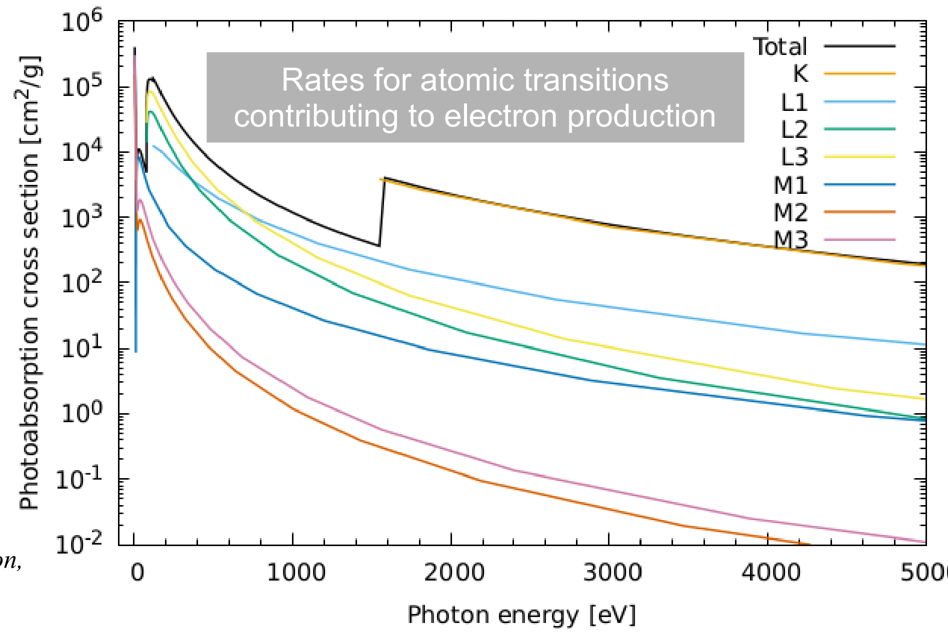

Progress in Geant4 Electromagnetic Physics Modelling and Validation,
J. Apostolakis et al, Journal of Physics 664, Nr 7, 072021 (2015)

Geant4 includes rates for the photo-ionization and atomic de-excitation processes fluorescence, Auger and Coster-Kronig electron emission.
Vacuum chamber material composition is defined in Geant4 input file.

Superposition of 300 Geant4 photon absorption events

E_{photon} = 30 eV

5-degree grazing angle

E_{photon} = 2000 eV

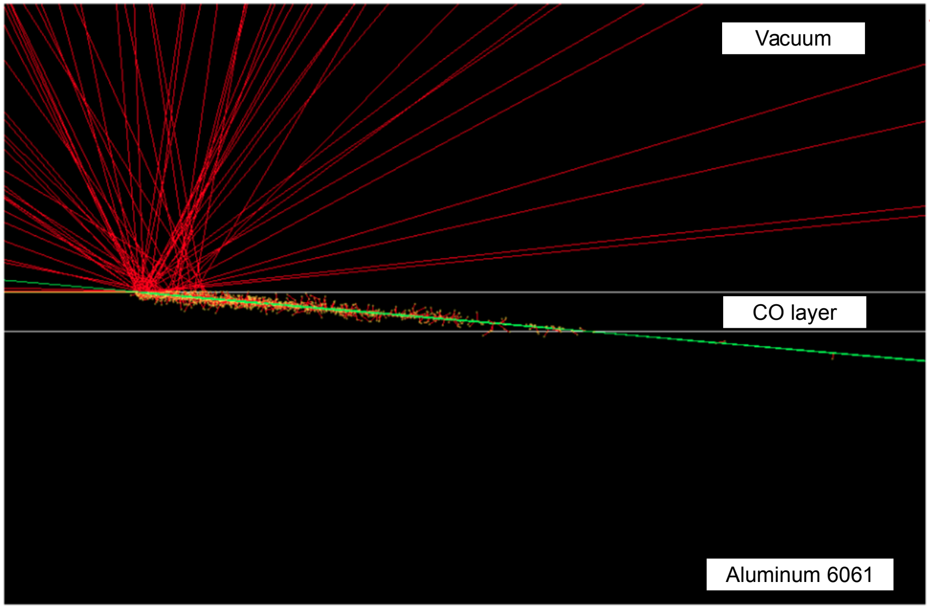

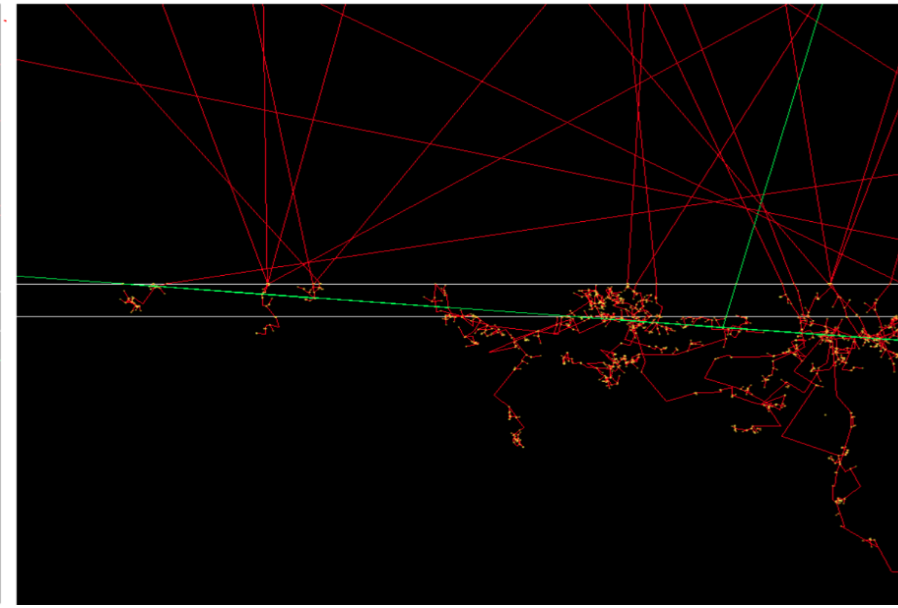

Zoom in on the 5-nm CO layer.
Low-energy photons interact predominantly in the CO layer.
High energy photons are absorbed most frequently in the aluminum

Two classes of final-state electrons can be distinguished: 1) photoproduced electrons with momenta which "remember" that of the photon. These enter the vacuum chamber at low energy via multiple scattering, and 2) electrons produced via atomi-de-excitation. These are emitted symmetrically and can carry high energy, i.e. the energy corresponding to the difference of atomic binding energy levels.

Electron production rates from Geant4 5.3 GeV e+ beam

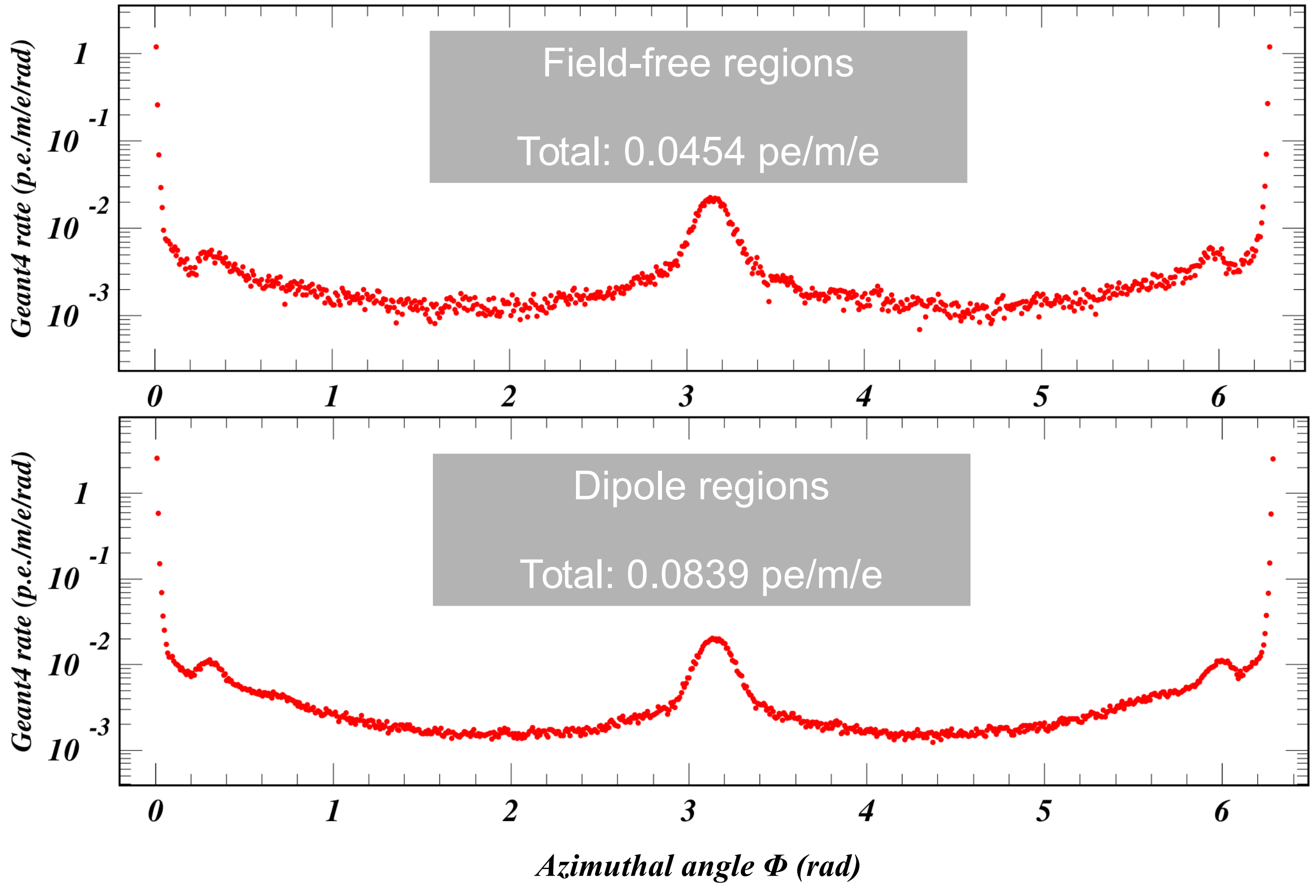

Number of electrons per beam particle per meter provided to electron cloud buildup modeling in 720 azimuthal location bins averaged over dipole and field-free regions separately.
These values replace the overall photon absorption rate and QE values used in the previous electron cloud buildup model.

Cornell University
Laboratory for Elementary-Particle Physics

Electron production energies 5.3 GeV e+ beam

Field-free regions

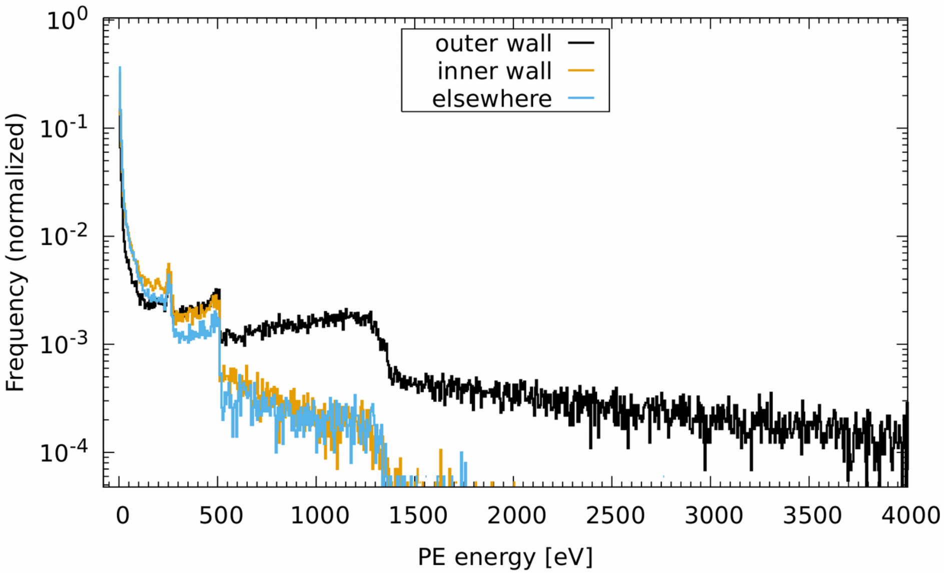

Dipole regions

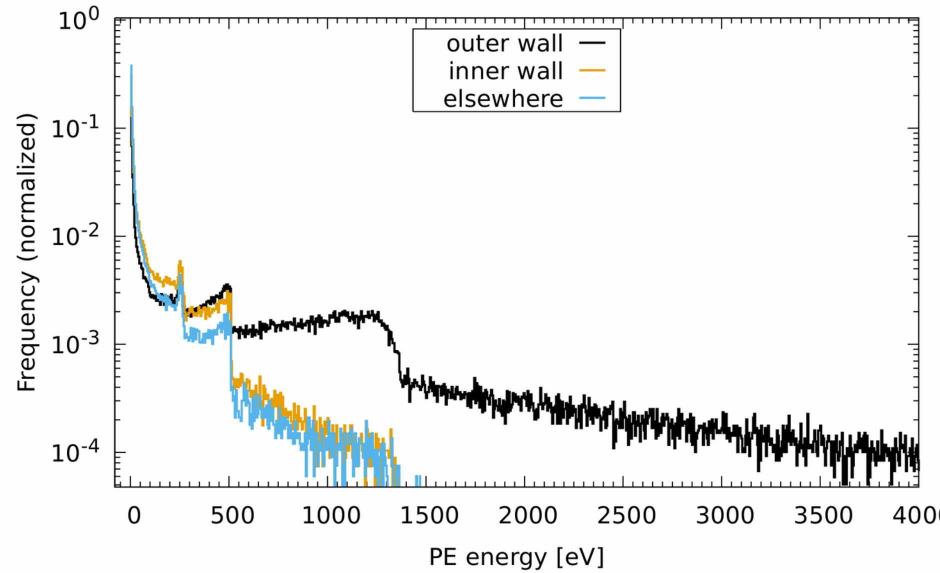

Strong dependence on azimuthal production location

Reflection selects low energy photons

Electron energy distributions provided to electron cloud buildup modeling for each of the three azimuthal regions separately for field-free and dipole regions of the ring

Summary

Improved measurements and data analysis for CESRTA beam dynamics motivated detailed modeling development

Photon tracking code updated with sophisticated vacuum chamber model

Geant4-based electron production model implemented as post-processor for photon tracking code

Combined model validated using CESRTA tune shift and beam size measurements (see STP Part 2)

Generalized implementation of means of choosing vacuum chamber surface properties and materials enables widespread applications

This work addresses the CESRTA project goal of providing validated modeling tools for present and future accelerator projects

Cornell University
Laboratory for Elementary-Particle Physics

Applications in progress

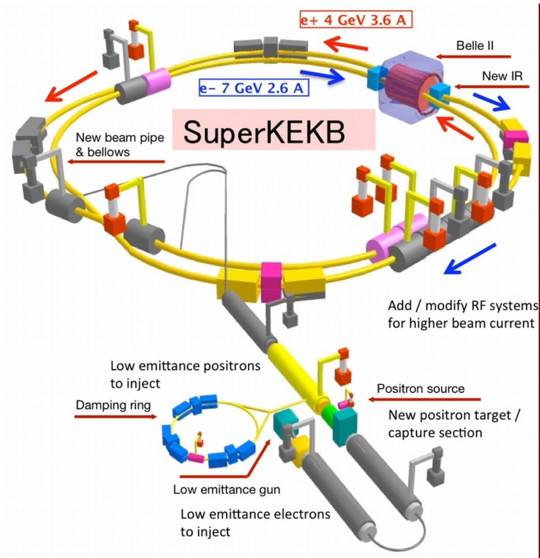

SuperKEKB

Phase 2 commissioning ended in July. Unexpectedly high rates of charged-particle background were observed in the interaction region.

We are responding to a request for calculations of high-energy photon rates incident on vacuum chamber walls in the interaction region.

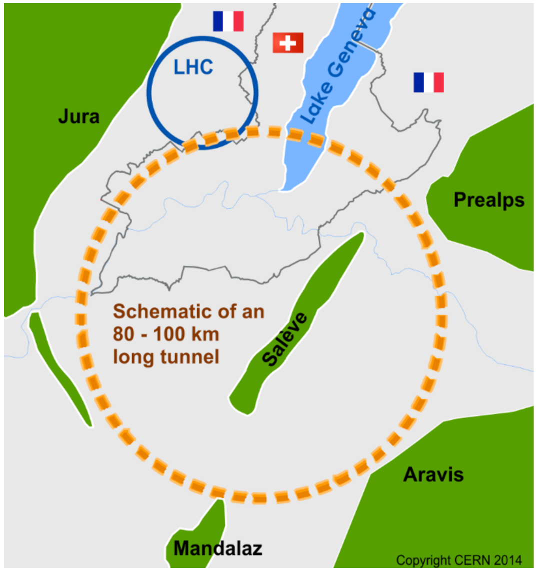

Future Circular Collider

A major design effort (Europe, US, Asia) will produce a conceptual design report in 2018. The existing vacuum design modeling for FCC-ee Z factory (98-km circumference, 46 GeV, NEG coating) assumes a seed cloud rather than seed electrons. Our code can test their assumptions.

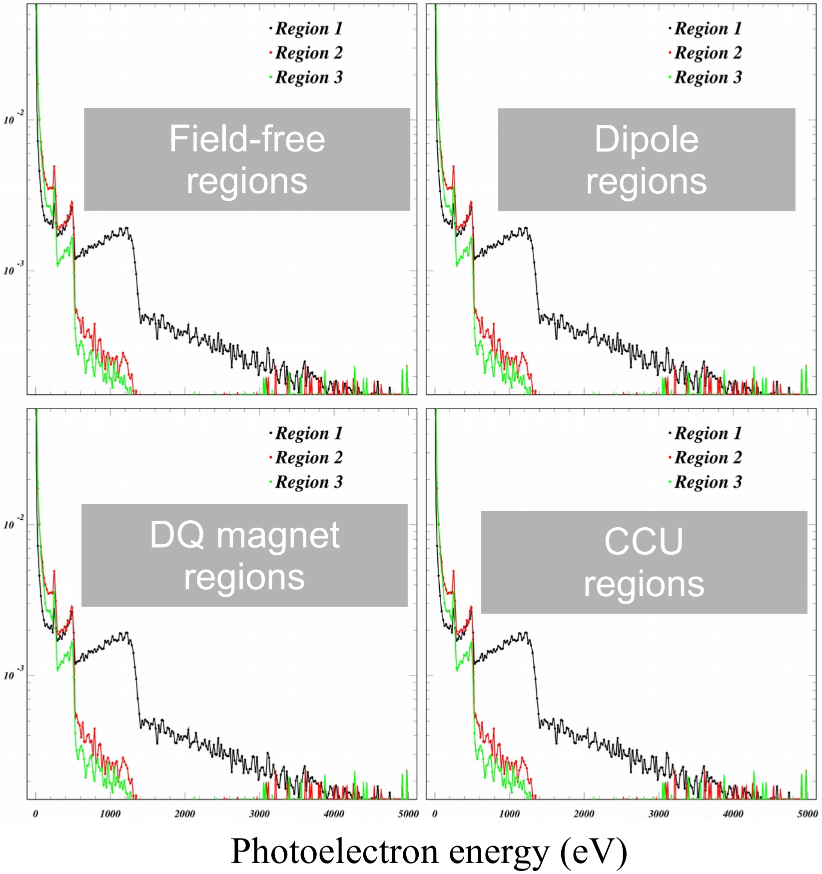

CHESS-U

Critical energy 50% higher brings additional atomic processes into play.
Interest in modeling cloud buildup in combined-function magnets and compact undulators as well as field-free and dipole regions.

Measurements and model validation of electron-cloud-induced betatron tune shifts in the CESRTA, CHESS and CHESS-U transition lattices and predictions for CHESS-U operation